Top Catal (2017) 60:869–878
DOI 10.1007/s11244-017-0751-y

ORIGINAL PAPER

Glass Beads Packed DBD-Plasma Assisted Dry Reforming of Methane

Debjyoti Ray[1] · P. Manoj Kumar Reddy[1] · Subrahmanyam Challapalli[1]

Published online: 10 April 2017

Abstract The aim of this work is to understand the effect of a packed bed dielectric barrier discharge for the transformation of greenhouse gases (CO_2 and CH_4) into value added products. Therefore, pure CH_4 and CO_2 have been introduced into the plasma discharge zone with the variation of feed flow rate, feed gas ratio and discharge power. It has been observed that at low flow rate of 20 mL/min (high residence time) the conversion of gases, selectivity and yield of products are higher, whereas, the optimum mole ratio of CH_4/CO_2 is 1.0. The activated species formed inside the plasma is diagnosed by emission spectroscopy. This study achieved 29% conversion of CH_4 and 21% conversion of CO_2 at SIE 6.4 J/mL with glass beads packed DBD, whereas energy efficiency has been found 1.75 mmol/kJ.

Keywords Dielectric barrier discharge · Residence time · Energy efficiency · Emission spectroscopy

1 Introduction

Even though H_2 has been recognized as the future fuel, its economical/ecofriendly production limits the practical applications. Traditionally, H_2 is produced from the fossil fuels, which are known to also produce greenhouse gases. In addition, to meet the demand for the desired H_2/CO, there is a need to develop alternative technologies of H_2 production. In this context, dry reforming, where co-processing of two potential greenhouse gases methane (CH_4) and carbon dioxide (CO_2) leading to the formation of syngas, appears to be a promising one [1, 2]. During the recent past, dry reforming has been receiving a great attention, due to the advantages that it involves the simultaneous conversion of two greenhouse gases CH_4 and CO_2, especially for low syngas (H_2/CO) ratio, desired syngas ratio, etc. [3, 4]. However, the thermo-catalytic dry reforming demands high temperature and catalyst also suffers a quick deactivation due to coke formation [5].

Dry reforming is more endothermic when compared to steam reforming and demands more energy [1]. Among the alternate methods of activating CO_2 and CH_4, non-thermal plasma (NTP) has advantageous like rapid initiation of the reaction, formation of high energy electrons that are capable of initiating the chemical reactions under mild reaction conditions and presence of multiple reactive species, etc. In addition, by integrating the discharge with a suitable catalyst/adsorbent, it is possible to improve the performance of the process. The advantage of a packed bed NTP is that it modifies the discharge characteristics and hence the overall performance [6–10]. Various NTP configurations were tested for DRM, namely atmospheric plasma jets [11], corona discharges [12], gliding arcs [13, 14] and dielectric barrier discharges (DBD) [3, 15, 16]. Among these plasmas, DBD has attracted a special attention, due to its advantages, such as the ability to produce a wide array of chemically reactive species under ambient conditions, uniform distribution of the discharge, high electron density etc. [6].

However, DBD dry reforming of CH_4 has disadvantages like the formation of undesired higher hydrocarbons (C_2–C_4), carbon/polymeric deposit and lower syngas ratio [5, 17]. In addition, the energy efficiency and selectivity towards the products is not satisfactory. Hence, a

✉ Subrahmanyam Challapalli
csubbu@iith.ac.in

[1] Department of Chemistry, Indian Institute of Technology Hyderabad, Hyderabad, Telangana 502 285, India

combination of heterogeneous catalyst with DBD plasma was attempted, to exploit the synergistic effect [18]. Various catalysts, such as Ni/γ-Al_2O_3, Cu/γ-Al_2O_3, Pd/γ-Al_2O_3, Ni-Cu/γ-Al_2O_3, Ag/γ-Al_2O_3, zeolite, La_2O_3/γ-Al_2O_3 etc., have been integrated and the plasma catalysis was tested for this reaction [5, 19–22]. Even though improvements are reported, the role of the catalyst/ surface is not clear. In addition, it is known that the discharge characteristics may be altered by integrating the discharge with porous/dielectric materials. With this background, the present study was focused on understanding the influence of glass beads (zero surface material) packing on DRM. The CH_4/CO_2 mole ratio has been varied from 1.0 to 2.0 and the total gas flow rate has been varied in order to obtain the best efficiency. Optical emission spectroscopy was used to identify the intermediates formed.

2 Experimental Set-Up

Figure 1 presents the experimental set-up used in the present study.

A co-axial cylindrical quartz tube with outer diameter 22 mm and inner diameter 19 mm was used to generate plasma. A stainless still rod of 10 mm diameter placed at the center of the quartz tube acts as the inner electrode, whereas a wire mesh wrapped around the quartz tube serves as the outer electrode (9 cm in length). The discharge gap was 4.5 mm and the resulting discharge volume is ~18.45 mL. Discharge was created by applying the AC high voltage and a capacitor (3 μF) was placed in between the ground and outer electrode.

The gas mixture (CH_4 and CO_2 without dilution) was sent through the DBD reactor and the total flow rate was varied between 20 and 40 mL/min by maintaining CH_4/CO_2 ratio as 1:2, 1:1, 1.5:1 and 2:1. The DBD plasma was operated by varying the AC voltage from 14 to 22 kV at a fixed frequency 50 Hz. The applied voltage was measured through a high voltage probe (Agilent 34136AHV probe), whereas a digital oscilloscope (Tektronix TDS2014B) was used to measure the charge–voltage (Q and V) signals. The discharge power and energy dissipated were calculated by using Q–V Lissajous method [23].

The reaction progress was monitored with a VARIAN 450 gas chromatograph (GC) equipped with two packed columns (Porapak Q and HAYESEP Q with 80/100 mesh, 2 m, 2 mm ID) connected in a series and a TCD detector and Ar carrier gas. The reactor outlet was connected to the GC inlet and analyzed at 15 min interval. An emission spectrometer (Princeton Instrument Action SpectraPro® SP-2300) equipped with three gratings (600 g/mm with 500 nm Blaze, 600 g/mm with 750 nm Blaze and 1200 g/mm with 500 nm Blaze) was used to collect the emission spectrum. The conversion, selectivity and yield of the major products, specific input energy (SIE) were calculated as follows:

$$\%\ \text{of}\ CH_4\ \text{conversion} = \left[1 - \frac{CH_4\ \text{outlet (mmol/min)}}{CH_4\ \text{inlet (mmol/min)}}\right] \times 100 \quad (1)$$

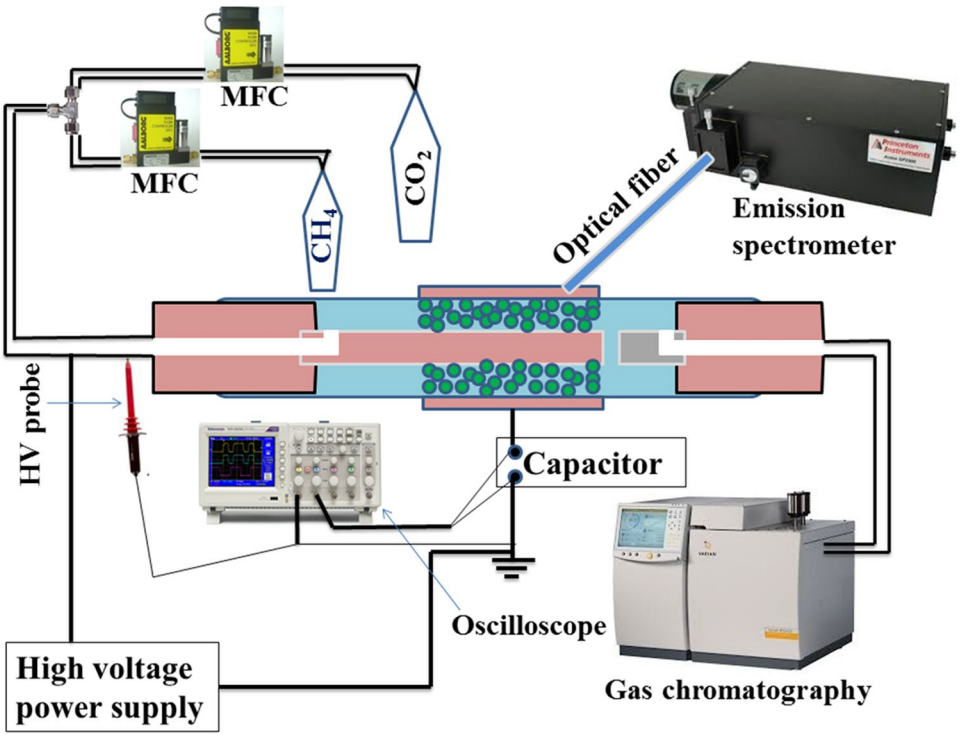

Fig. 1 Schematic diagram of experimental set-up

$$\%\ \text{of}\ CO_2\ \text{conversion} = \left[1 - \frac{CO_2\ \text{outlet (mmol/min)}}{CO_2\ \text{inlet (mmol/min)}}\right] \times 100 \quad (2)$$

$$\%\ \text{of}\ H_2\ \text{selectivity} = \frac{H_2\ \text{produced (mmol/min)}}{2 \times C H_4\ \text{converted (mmol/min)}} \times 100 \quad (3)$$

$$\%\ \text{of CO selectivity} = \frac{\text{CO produced (mmol/min)}}{CH_4\ \text{converted (mmol/min)} + CO_2\ \text{converted (mmol/min)}} \times 100 \quad (4)$$

$$\%\ \text{of}\ H_2\ \text{yield} = \frac{H_2\ \text{produced (mmol/min)}}{2 \times CH_4 \text{input (mmol/min)}} \times 100 \quad (5)$$

$$\%\ \text{of CO yield} = \frac{\text{CO produced (mmol/min)}}{CH_4\ \text{input (mmol/min)} + CO_2\ \text{input (mmol/min)}} \times 100 \quad (6)$$

$$\text{SIE (J/mL)} = \frac{\text{Power (W)}}{\text{Total gas flow rate (mL/min)}} \times 60 \quad (7)$$

The H_2/CO mole ratio and carbon balance (based on major products) have been calculated as:

$$\frac{H_2}{CO} = \frac{H_2\ \text{produced (mmol/min)}}{\text{CO produced (mmol/min)}} \quad (8)$$

$$\%\ \text{of carbon balance} = \frac{[CH_4]_{out} + [CO_2]_{out} + [CO]_{out}}{[CH_4]_{in} + [CO_2]_{in}} \times 100 \quad (9)$$

The total energy efficiency of plasma dry reforming reaction according to the conversion of reactants (CH_4 & CO_2) has been defined as:

$$E(\text{mmol/kJ}) = \frac{CH_4\ \text{converted (mol/min)} + CO_2\ \text{converted (mol/min)}}{60 \times \text{discharge power (W)}} \quad (10)$$

3 Result and Discussion

3.1 Physical Characteristics of Discharges

The electrical signals of the DBD with and without packing at a fixed discharge power of 0.8 W are shown in Fig. 2. In the case of glass beads packing, the discharge is due to both conventional surface discharge and weak microdischarges inside the plasma region [24]. It is worth mentioning that glass beads packing improves the discharge strength, as the applied voltage required, to keep constant a discharge

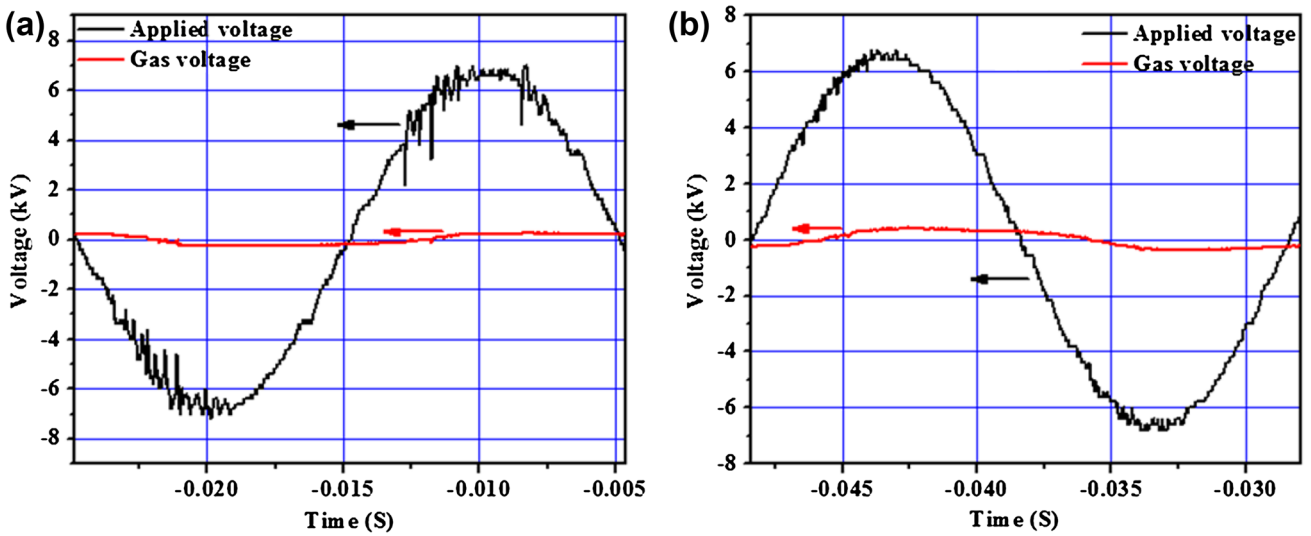

Fig. 2 Electrical signals of dry reforming reaction at discharge power 0.8 W **a** without packing; **b** glass beads packing

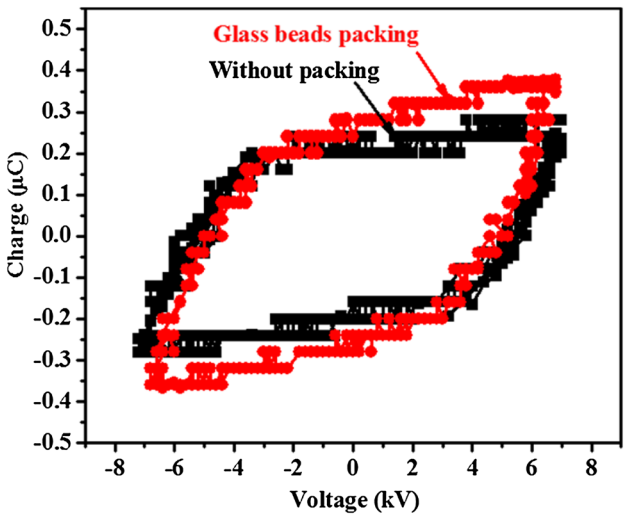

Fig. 3 Lissajous figures for dry reforming system at discharge power 0.8 W

Table 1 Electrical parameters of DBD at a fixed discharge power (0.8 W) for without and glass beads packed system

Packed materials	Applied voltage pk–pk (kV)	Breakdown voltage (kV)	Charge transferred per half cycle (μC)
No pack	15.4	5.4	0.45
Glass beads	14	4.7	0.53

power of 0.8 W is about 10% lower than that of DBD reactor without packing. DBD shows discharge power 0.8 W at applied voltage 15.4 kV_{pk-pk} that decreased to 14 kV_{pk-pk} upon glass beads packing. It may be due to dielectric heating. Figure 3 shows the shape change of Lissajous figure on integrating glass beads with the discharge. Table 1 summarizes the gas breakdown voltage and charge transferred per half cycle, which confirms the decrease in the breakdown voltage from 5.4 to 4.7 kV for the packed bed DBD. This is due to the change in discharge mode from a typical filamentary to a combination of surface discharge and filamentary weak microdischarge and the lower breakdown voltage is due to the improved filed strength on the surface of the glass beads [5]. In addition, it was observed that the transferred charge for the half cycle also increased from 0.45 μC (without packing) to 0.53 μC (glass beads DBD). A similar observation was reported by Tu et al. for Ni/Al_2O_3 packing [5].

3.2 Effect of CH_4/CO_2 Mole Ratio on Dry Reforming Reaction

Figure 4 presents the effect of CH_4/CO_2 mole ratio on the performance of the packed bed DBD during DRM. As seen from Fig. 4, conversion of CH_4 decreases with increasing CH_4/CO_2 mole ratio (at a fixed flow rate), whereas, conversion of CO_2 increases with the increasing CH_4/CO_2 mole ratio. Figure 4b shows the effect of CH_4/CO_2 mole ratio on the selectivity of major products, which also confirms the improved selectivity with packed DBD. H_2 selectivity increases with CH_4/CO_2 mole ratio from 0.5 to 2.0, whereas, CO selectivity decreases and the highest CO selectivity (62%) was observed at CH_4/CO_2 ratio 1.0. The relation between products yield and CH_4/CO_2 mole ratio is shown in Fig. 4c. The yield of major products decreases with the increase of CH_4/CO_2 mole ratio and glass beads packed DBD shows higher yield compared to DBD without packing. Figure 4d presents the effect of CH_4/CO_2 mole ratio on the production of syngas (H_2/CO), which shows that H_2/CO ratio increases with the increasing CH_4/CO_2 ratio.

3.3 Effect of Total Gas Flow Rate on Dry Reforming Reaction

Figure 5a represents the effect of the gas flow rate on the performance of DBD during dry methane reforming. The conversion of methane decreases from 33 to 29% with increasing flow rate from 20 to 40 mL/min, at 3.2 W and CH_4/CO_2 ~1.0. This decrease is due to the decrease in the residence time from 0.92 to 0.46 min. As a result, the conversion of CO_2 also decreased from 28 to 21% with the increasing of flow rate from 20 to 30 mL/min and slightly increased to 22% at the flow rate 40 mL/min. Figure 5b, c shows the selectivity and yield of the major products that also indicated decreasing selectivity with increasing flow rate. H_2 selectivity decreased from 43 to 20% when the gas flow rate increased from 20 to 40 mL/min similarly the yield also decreases from 14 to 6% under the same conditions. The CO selectivity and yield also decreased from 78 to 39% and 24 to 10%, respectively with the increasing the total gas flow rate from 20 to 40 mL/min. The H_2/CO mole ratio and carbon balance with flow rate are shown in Fig. 5d. The carbon balance decreased with the increasing of gas flow rate, indicating that carbon formation is favorable at higher flow rate. The best H_2/CO ratio achieved 0.74 at 30 mL/min flow rate.

3.4 Effect of Discharge Power or SIE on Dry Reforming Reaction

Figure 6a presents the conversion of reactants with respect to discharge power at 30 mL/min and CH_4/CO_2 mole ratio 1.0. The conversion of reactants increases with the increasing discharge power. It is worth mentioning that the glass beads packed DBD showed higher conversion than DBD reactor without packing, probably due to higher dielectric

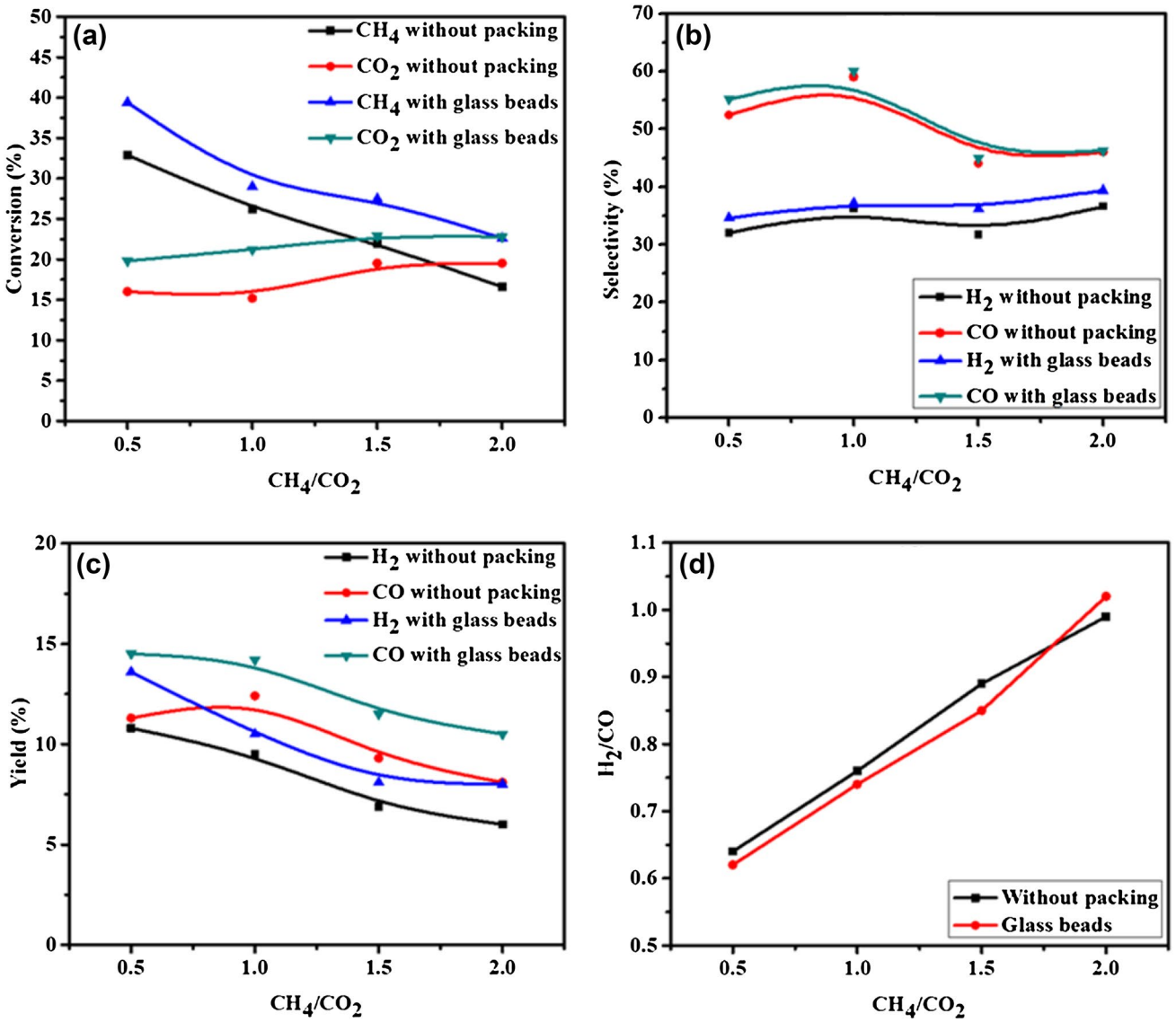

Fig. 4 Effect of CH_4/CO_2 mole ratio: **a** conversion, **b** selectivity, **c** yield, **d** H_2/CO ratio. (Total gas flow rate 30 mL/min, discharge power 3.2 W, frequency 50 Hz)

constant of glass beads (4.1) which increases the electrical filed strength at the contact points. The important observation is that CH_4 conversion is higher than that of CO_2, whereas, thermo-catalytic dry reforming repots higher conversion of CO_2 [25, 26].

In this study, 29 and 21% conversion of CH_4 and CO_2 was achieved with glass beads packed DBD at 3.2 W, respectively. The yield of major products with respect to specific input energy (SIE) is shown in Fig. 6b, which confirms the increasing product yield with SIE. Interestingly, CO yield is more than H_2 yield, indicating the formation of higher carbon products. The highest CO and H_2 yield observed was 14.2 and 10.8%, respectively. Figure 6c shows the selectivity of major products with variation of SIE. The selectivity of major products decreased with the increase of SIE and the CO shows more selectivity than H_2. The glass beads packed DBD shows almost 62 and 38%, selectivity towards CO and H_2 respectively.

3.5 Syngas Production and Carbon Balance in Dry Reforming Process

Figure 7 presents the influence of discharge power on the syngas selectivity at different CH_4/CO_2 mole ratios.

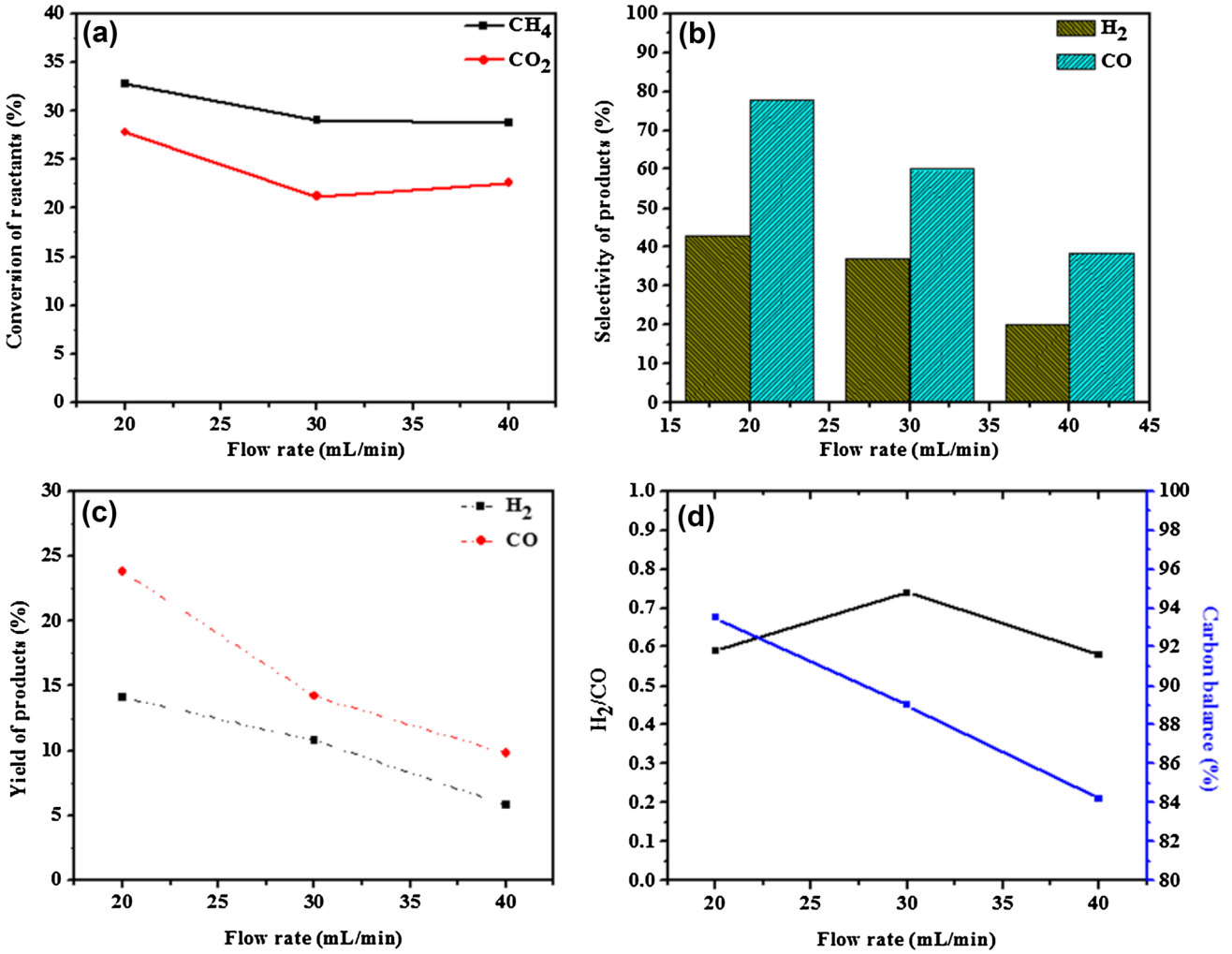

Fig. 5 Effect of feed flow rate on the dry reforming reaction **a** conversion of reactants; **b** selectivity of major products; **c** yield of major products; **d** H_2/CO ratio and carbon balance. (Discharge power 3.2 W, frequency 50 Hz, $CH_4/CO_2 = 1.0$, glass beads packed)

As seen in Fig. 7, the H_2/CO ratio remains almost constant and without packed DBD shows higher H_2/CO ratio. The maximum H_2/CO ratio observed was 1.02 for glass beads packed DBD at CH_4/CO_2 mole ratio 2.0 which is nearly the same as that of DBD with no packing (0.99). It is observed that H_2/CO ratio is more at higher CH_4/CO_2 mole ratio due to the excess formation of H_2 and H_2/CO ratio increases with the increasing CH_4/CO_2 mole ratio from 0.5 to 2.0. This observation indicates that the syngas ratio can be controlled by adjusting the CH_4/CO_2 mole ratio [13]. Generally, it is believed that Eq. 11 is responsible for lower H_2/CO ratio. The deposited carbon may also influence for decreasing H_2/CO ratio via reverse Boudouard reaction (Eq. 12) [1, 13]. In this study the H_2/CO ratio found was ~1.0 suggesting that the both Eqs. 11 and 12 may lead to high CO_2 conversion, but low H_2/CO ratio.

$$CO_2 + H_2 \rightarrow CO + H_2O \quad (11)$$

$$CO_2 + C_{(S)} \rightarrow 2CO \quad (12)$$

The carbon balance based on the major gas products in DBD dry reforming reaction is shown in Fig. 8a. For both with and without packing, the carbon balance was above 90% and packed bed DBD showed the lowest carbon balance. Glass beads packing increases the strength of microdishcarges, and favors carbon/higher hydrocarbon formation. Figure 8b shows the carbon formation with the variation of CH_4/CO_2 mole ratio in glass beads packed system. The result indicated the poor carbon balance at high CH_4/CO_2.

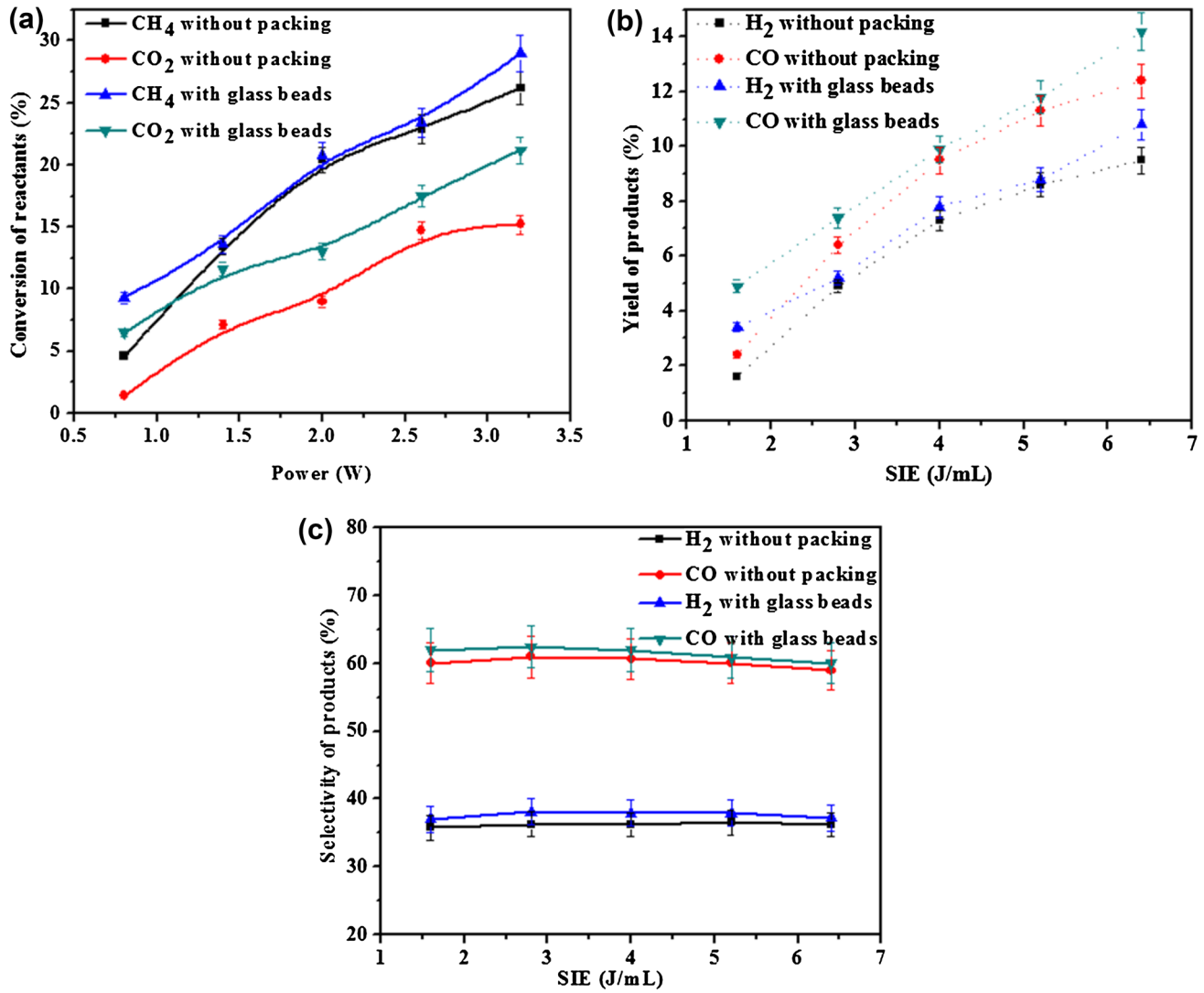

Fig. 6 **a** Conversion as a function of the discharge power, **b** yield of major products with the variation of SIE; **c** selectivity of major products with the variation of SIE (total gas flow rate 30 mL/min, CH_4/CO_2 mole ratio 1.0)

3.6 Energy Efficiency

Figure 9 presents the energy efficiency (calculated by using Eq. 10) of dry reforming reaction under the experimental conditions of the present study. It has been observed that energy efficiency decreases with increasing power/specific input energy, as shown in Fig. 9a. Glass beads packed DBD showed 1.75 mmol/kJ at SIE 6.4 J/mL whereas for DBD alone, it was 1.44 mmol/kJ. The best energy efficiency of 2.2 mmol/kJ was achieved at SIE 1.6 J/mL with glass beads packed DBD. Table 2 compares the energy efficiency of various DBD reactors reported in the literature for this reaction. Figure 9b shows the energy efficiency with the variation of CH_4/CO_2 mole ratio at different powers at a constant total feed flow rate 30 mL/min. The highest efficiency observed at CH_4/CO_2 ratio1.5. Figure 9c represents the variation of energy efficiency with the feed flow rate at 3.2 W for glass beads packed DBD. The energy efficiency increases almost linearly with the increase of feed flow rate. ~2.38 mmol/kJ was achieved at 3.2 W in 40 mL/min flow rate with glass beads DBD reactor.

3.7 Optical Emission Spectroscopy

The optical emission spectra are shown in Fig. 10. The signature peaks of the activated species, such as CO, CH, CO_2^+, OH, identified from the emission spectra are

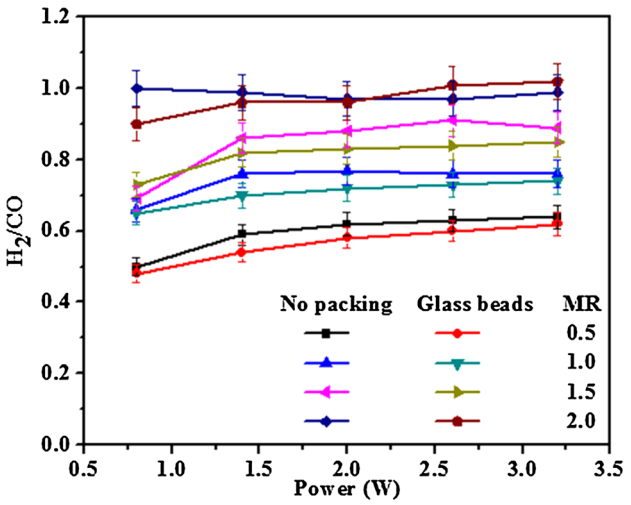

Fig. 7 Influence of power on syngas ratio (H_2/CO) for different CH_4/CO_2 mole ratio with and without packed DBD dry reforming reaction. (Total flow rate 30 mL/min, frequency 50 Hz)

shown in Fig. 10 [23]. The signature peaks due to CH ($C^2\Sigma^+ \rightarrow X^2\Pi$, 314 nm and $B^2\Sigma^- \rightarrow X^2\Pi$, 390 nm) indicated the formation of hydrocarbons (Fig. 10a) [18]. The peak centered at 297 nm is due to the transition of $b^3\Pi^+ \rightarrow a^3\Pi$ of CO, whereas, the emission of CO_2 is at 335 and 375 nm [23]. An intense peak at 356 nm is due to $OH^{+,\ 3}\Pi \rightarrow {}^3\Sigma$ (0,0) transition [28], indicates the formation of liquid by products. The peak corresponding to 400.53 and 406.52 nm is due to the transition of $C^3\Delta_u \rightarrow a^1\Delta_g$ and $A^3\Sigma_{u+} \rightarrow X^3\Sigma_{g-}$ respectively [29]. Figure 10b represents the visible region of the emission spectra. Here the peak found around at 450 nm, 520 nm ($B^1\Sigma \rightarrow A^1\Pi$) and 561 nm that confirms the formation of major product CO [4, 29]. The CO_2^+ peak observed at 413.60 nm is due to the transition of $A^2\Pi \rightarrow X^2\Pi$. A small peak centered around 588.28 nm is due to the O_2^+ ($b^4\Pi_g^- \rightarrow a^4\Pi_u$), whereas, activated CO showed a peak at 483 nm [28, 29]. A small shoulder peak at 431 nm is due to CH ($A^2\Delta \rightarrow X^2\Pi$, $\Delta\nu = 0$) transition [18].

4 Conclusions

Non-thermal Plasmas are efficient for transformation of greenhouse gases into value added products. The interactions of glass beads with plasma improves the performance of DBD plasma for the dry reforming reaction. Typical results showed that, glass beads packing improves the discharge strength, decreases the breakdown voltage and increases transferred charge for the half cycle when compared to the DBD reactor without packing. During the dry reforming, CH_4 conversion decreases with increasing CH_4/CO_2 mole ratio, compared to unpacked reactor packed bed reactor increased CH_4 conversion 11% and CO_2 conversion to 38% at 1:1 mole ratio with highest discharge power. Increasing the flow rate, the conversion of CH_4 and the selectivity and yield of the major products decreased. The carbon balance also decreased with increasing power. The packed bed DBD showed the lowest carbon balance. This is a sign of higher hydrocarbons formation. Energy efficiency decreases with increasing power or SIE, packed bed reactor

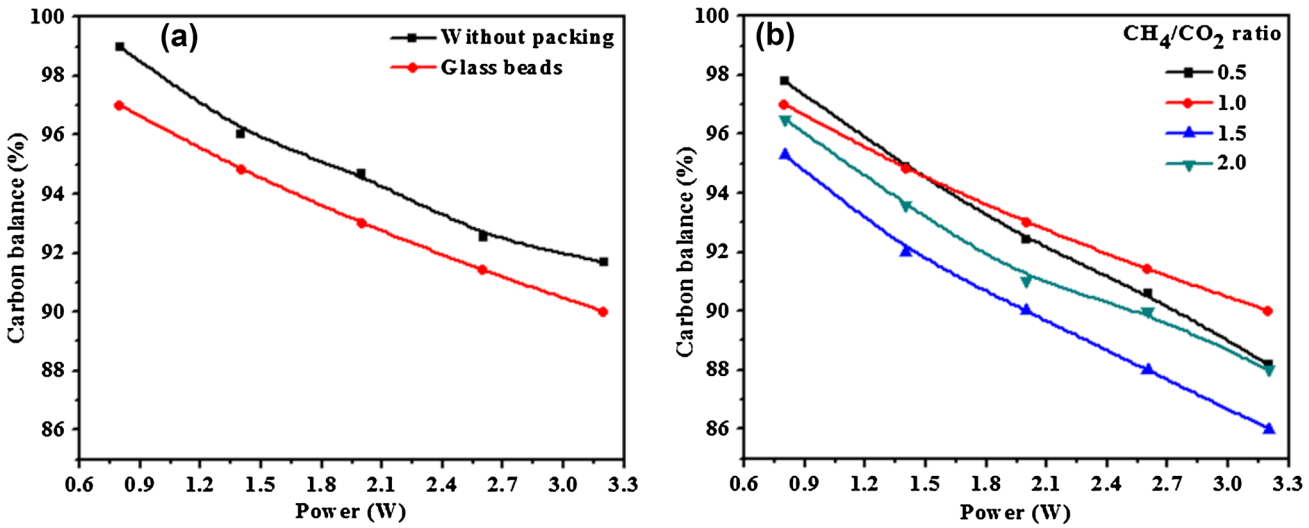

Fig. 8 Influence of power on carbon balance of DBD based dry reforming reaction **a** at CH_4/CO_2 mole ratio 1.0 (comparison between without packed and packed DBD), **b** with glass beads packed (variation of mole ratio)

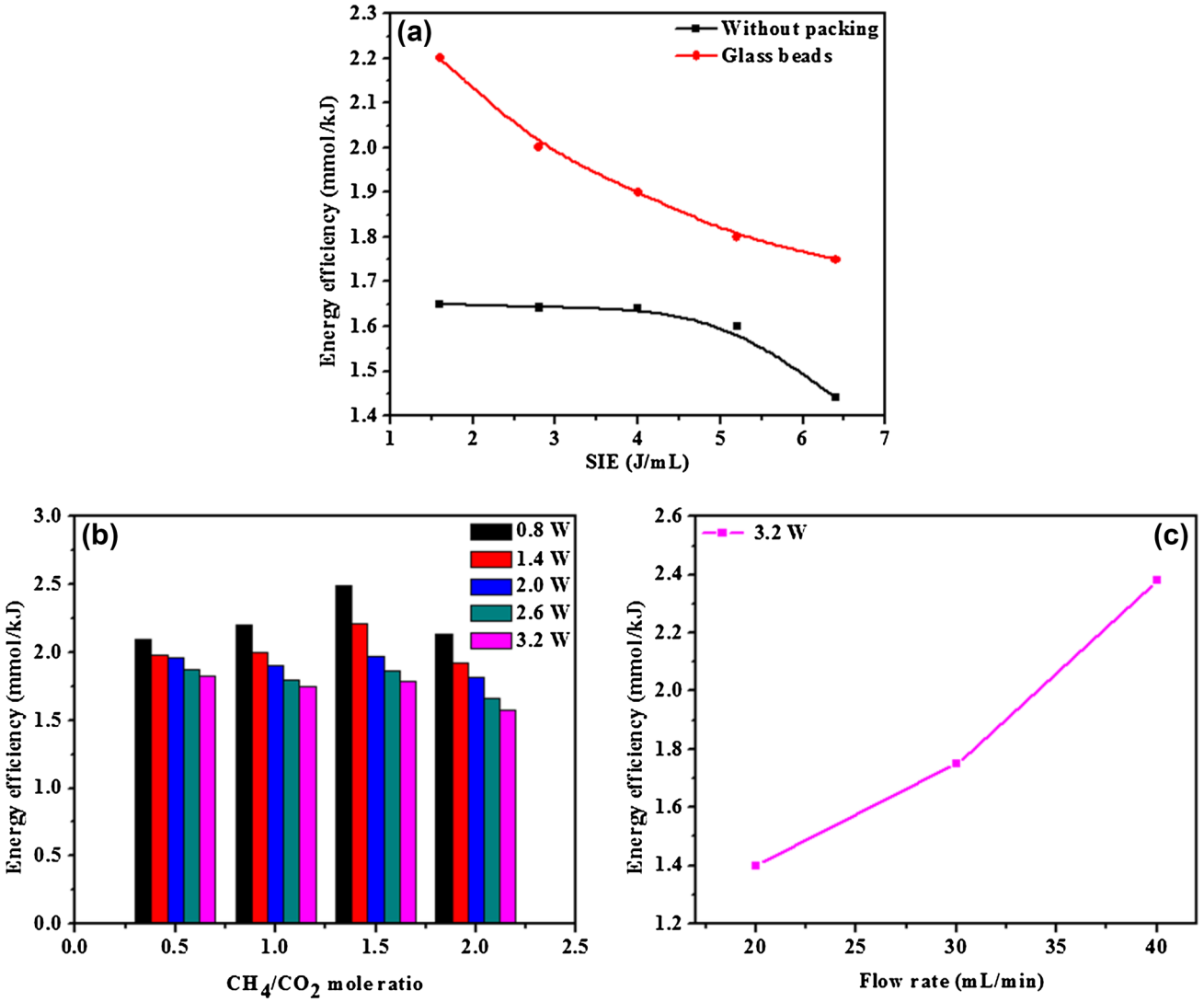

Fig. 9 Energy efficiency of dry reforming reaction **a** with the variation of SIE (total flow rate 30 mL/min, $CH_4/CO_2 = 1.0$, frequency 50 Hz); **b** with the variation of CH_4/CO_2 mole ratio (glass beads packed, total flow rate 30 mL/min, frequency 50 Hz); **c** with the variation of different flow rate (glass beads packed, $CH_4/CO_2 = 1.0$, discharge power 3.2 W, frequency 50 Hz)

Table 2 Comparison of conversion, product selectivity, H_2/CO mole ratio and energy efficiency for dry reforming reaction using DBD plasma

Plasma	CH_4/CO_2	Power (W)	Packed material	Total gas flow rate (mL/min)	Conversion (%)		Selectivity (%)		H_2/CO	E (mmol/kJ)	References
					CH_4	CO_2	H_2	CO			
DBD	2.0	100	–	60	64.3	43.1	–	32.2	~1.8	0.26	[27]
DBD	1.0	50	10% Ni/Al_2O_3	50	56.4	30.2	31	52.4	–	0.32	[18]
DBD	1.0	97	26% Ni/Al_2O_3	50	18	12.5	45	24	~2.4	0.033	[5]
DBD	1.0	75	–	60	40	25	40	–	~0.85	0.19	[19]
DBD	1.0	7.5	10% Ni/Al_2O_3	50	19.6	9.3	34	37.5	~1.2	0.72	[6]
DBD	2.0	3.33	20% Ni/Al_2O_3	40	49	31	56	35	2.25	0.55	[3]
DBD	1.0	3.2	Glass beads	30	29	21.2	37.2	60	0.74	1.75	This work

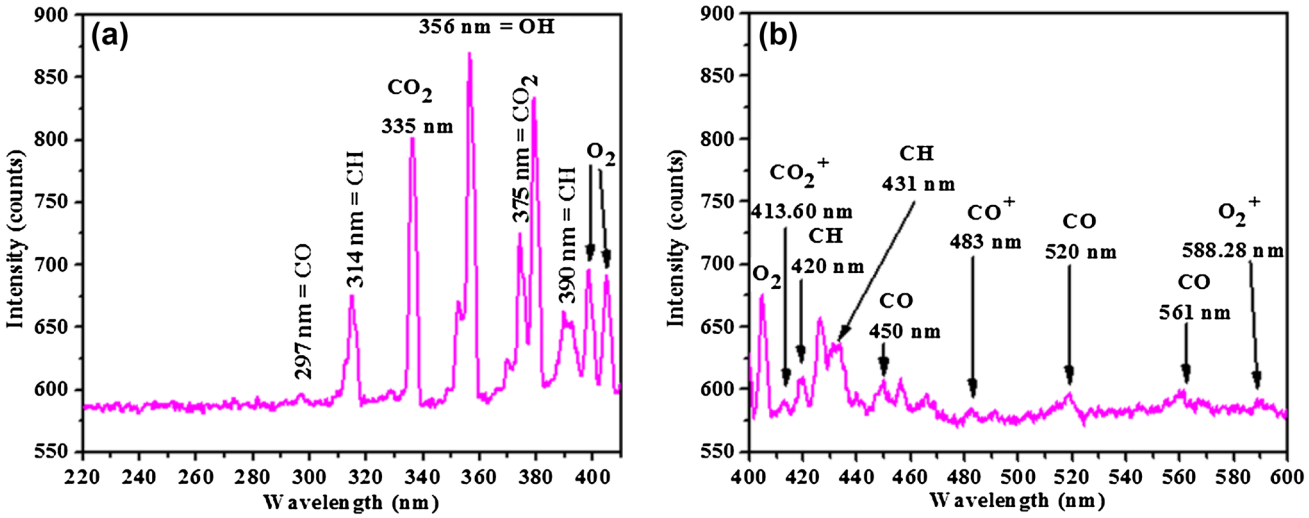

Fig. 10 Emission spectra of dry reforming reaction **a** intensity range 220–450 nm; **b** intensity range 400–600 nm. (Applied voltage 18 kV, grating: 600 glue at 500 nm, glass beads packed DBD)

showed 1.75 mmol/kJ and unpacked reactor showed 1.44 mmol/kJ at SIE of 6.4 J/mL.

Acknowledgements The authors would like to acknowledge the funding supporter Ministry of New and Renewable Energy (MNRE), New Delhi, India (project No. CHY/2014-15/019/MNRE/CHS/0140). Debjyoti is thankful to UGC India for providing fellowship.

References

1. Pawar V, Ray D, Subrahmanyam C, Janardhanan VM (2015) Energy Fuels 29:8047
2. Nozaki T, Tsukijihara H, Fukui W, Okazaki K (2007) Energy Fuels 21:2525
3. Mahammadunnisa S, Manoj Kumar Reddy P, Ramaraju B, Subrahmanyam C (2013) Energy Fuels 27:4441
4. Kameshima S, Tamura K, Ishibashi Y, Nozaki T (2015) Catal Today 256:67
5. Tu X, Gallon HJ, Twigg MV, Gorry PA, Whitehead JC (2011) J Phys D 44:274007
6. Zeng Y, Zhu X, Mei D, Ashford B, Tu X (2015) Catal Today 256:80
7. Mahammadunnisa S, Reddy EL, Ray D, Subrahmanyam C, Whitehead JC (2013) Int J Greenh Gas Control 16:361
8. Mahammadunnisa S, Manoj Kumar Reddy P, Linga Reddy E, Subrahmanyam C (2013) Catal Today 211:53
9. Linga Reddy E, Biju VM, Subrahmanyam C (2012) Appl Energy 95:87
10. Mahammadunnisa S, Manoj Kumar Reddy P, Subrahmanyam C (2014) RSC Adv 4:4034
11. Li X, Tao X, Yin Y (2009) IEEE Trans Plasma Sci 37(6):759
12. Li MW, Tian YL, Xu GH (2007) Energy Fuels 21:2335
13. Tu X, Whitehead JC (2014) Int J Hydrog Energy 39:9658
14. Rueangjitt N, Sreethawong T, Chavadej S, Sekiguchi H (2009) Chem Eng J 155:874
15. Snoeckx R, Zeng YX, Tu X, Bogaerts A (2015) RSC Adv 5:29799
16. Wang Q, Yan BH, Jin Y, Cheng Y (2009) Plasma Chem Plasma Process 29:217
17. Goujard V, Tatibouët JM, Batiot-Dupeyrat C (2009) Appl Catal A 353:228
18. Tu X, Whitehead JC (2012) Appl Catal B 125:439
19. Zhang AJ, Zhu AM, Guo J, Xu Y, Shi C (2010) Chem Eng J 156:601
20. Sentek J, Krawczyk K, Młotek M, Kalczewska M, Kroker T, Kolb T, Schenk A, Gericke KH, Schmidt-Szałowski K (2010) Appl Catal B 94:19
21. Pham MH, Goujard V, Tatibouet JM, Batiot-Dupeyrat C (2011) Catal Today 171:67
22. Gallon HJ, Tu X, Whitehead JC (2012) Plasma Process Polym 9:90
23. Ray D, Subrahmanyam C (2016) RSC Adv 6:39492
24. Mei D, Zhu X, He YL, Yan JD, Tu X (2015) Plasma Sources Sci Technol 24:015011
25. Wang N, Qian W, Chu W, Wei F (2016) Catal Sci Technol. doi:10.1039/c5cy01790d.
26. Zhang L, Zhang Y (2015) RSC Adv 5:62173
27. Zhang Y, Li Y, Wang Y, Liu C, Eliasson B (2003) Fuel Process Technol 83:101
28. Kraus M, Egli W, Haffner K, Eliasson B, Kogelschatz U, Wokaun A (2002) Phys Chem Chem Phys 4:668
29. Garcia-Cosio G, Calixto-Rodriguez M, Martinez H (2009) 29th ICPIG, Cancún, México, July 12–17, Topic number B6